encit 2020

ABCM Associação Brasileira de Engenharia e Ciências Mecânicas

18th Brazilian Congress of Thermal Sciences and Engineering
November 16–20, 2020 (Online)

ENC-2020-0151
OPTIMIZATION OF THERMAL ABLATION OF BIOLOGICAL TISSUES WITH HIGH INTENSITY FOCUSED ULTRASOUND

Rodrigo L. S. Silva
Mohsen Alaeian
Helcio R. B. Orlande
Federal University of Rio de Janeiro, Department of Mechanical Engineering, PEM/COPPE, Rio de Janeiro, RJ, 21945-970, Brazil
rodrigo.silva@mecanica.coppe.ufrj.br
mohsen@mecanica.coppe.ufrj.br
helcio@mecanica.coppe.ufrj.br

Abstract. *In clinical applications, thermal ablation consists of removal or destruction of a specific tissue by heat. Different heat sources can be used to increase the temperature of biological tissues during thermal ablation. High Intensity Focused Ultrasound (HIFU) is a non-invasive thermal ablation technique that has minimal or no side-effects. In this study, a numerical simulation of the HIFU treatment of a tumor was developed, aiming at predicting the necrotic tissue region. The acoustic problem was simulated with the numerical solution of the mass and momentum conservation equations. The temperature field was obtained by solving Pennes' bioheat equation with the finite difference method, by neglecting bubble dynamics and cavitation effects, followed by the calculation of the thermal damage. The size, shape and location of the necrotic tissue were predicted, for specific transducer heating rate and heating time, which were required for the thermal ablation of the desired region. The numerical solution obtained in this work was verified with the analytical solution of a similar problem in an homogeneous medium. The thermal ablation process was then optimized under uncertainties in the model parameters by using the Markov chain Monte Carlo method.*

Keywords: *high intensity focused ultrasound, thermal ablation, optimization under uncertainties, Markov chain Monte Carlo method*

1. INTRODUCTION

Thyroid nodules are relatively common, and in many cases they are benign, do not cause any relevant symptoms and only require clinical follow-up. On the other hand, there are cases in which the nodule grows and results in a series of complications, thus requiring a more specific treatment (Haugen *et al.*, 2016; Tunbridge *et al.*, 1977; Vander *et al.*, 1968). Surgical procedures are usually recommended for the treatment of these nodules, but they may cause undesirable effects such as hypothyroidism, bleeding and infections.

High Intensity Focused Ultrasound (HIFU) treatment consists in using a concave spherical ultrasound transducer, which enables the concentration of the acoustic energy in a specific region. This energy concentration increases the tissue temperature, allowing a minimally invasive thermal ablation treatment without relevant side effects (Hill and Ter Haar, 1995; Kennedy *et al.*, 2003).

This work aims at the optimization of the thermal ablation treatment of a tumor, by considering uncertainties in the model parameters and in the acceptable optimal solution. The Markov chain Monte Carlo method, implemented via the Metropolis-Hastings algorithm (Kaipio and Fox, 2011; Kaipio and Somersalo, 2006; Metropolis *et al.*, 1953), was used as the optimization procedure. Although the main objective of this work is the treatment of thyroid nodules, an idealized two-dimensional rectangular region is examined for the preliminary results presented below.

2. ACOUSTIC PROBLEM

For the modeling of the acoustic waves propagating inside the medium, classical hypotheses include small field fluctuations, negligible energy dissipation and no body forces. For a linear problem in a homogeneous medium, mass conservation and momentum equations can be written as (Kinsler *et al.*, 1999):

$$\frac{\partial \rho}{\partial t} + \rho_0 \nabla \cdot \mathbf{v} = 0 \tag{1}$$

$$\frac{\partial \mathbf{v}}{\partial t} + \frac{1}{\rho_0} \nabla p = 0 \tag{2}$$

where the relation between the acoustic pressure and density is given by the following equation of state (Kinsler *et al.*, 1999):

$$p = c_0^2 \rho \tag{3}$$

In the case of a HIFU treatment, the tissue temperature increase occurs due to the energy absorption. Therefore, energy dissipation must be taken into account. In addition, the concentrated absorption of the acoustic energy results in very large pressure amplitudes, and nonlinear effects can be significant (Hill and Ter Haar, 1995; Khokhlova *et al.*, 2006).

The k-Wave MATLAB toolbox (Treeby and Cox, 2010), which was used in this work, models the attenuation by the power law, according to equation (4). In this model, a is the attenuation per unit length, a_0 is the power law prefactor and z is the power law exponent (Szabo, 1995).

$$a = a_0 (2\pi f_0)^z \tag{4}$$

The equations solved by k-Wave are given by (5), (6) and (7). These equations represent, for a heterogeneous medium with energy dissipation, conservation of mass and momentum, as well as a relation between the acoustic pressure and density (Treeby *et al.*, 2012), respectively.

$$\frac{\partial \rho}{\partial t} + (2\rho + \rho_0) \nabla \cdot \mathbf{v} + \mathbf{v} \cdot \nabla \rho_0 = 0 \tag{5}$$

$$\frac{\partial \mathbf{v}}{\partial t} + \frac{1}{\rho_0} \nabla p = 0 \tag{6}$$

$$p = c_0^2 \left(\rho + \mathbf{d} \cdot \nabla \rho_0 + \frac{B}{2A} \frac{\rho^2}{\rho_0} - J\rho \right) \tag{7}$$

In the acoustic formulation, $\mathbf{d}$ represents the particle displacement, B/A is the nonlinearity parameter, and J, represented by (8), is a particular operator that considers the attenuation (Treeby *et al.*, 2012).

$$J = -2a_0 c_0^{z-1} \frac{\partial}{\partial t} \left(-\nabla^2\right)^{\frac{z}{2}-1} + 2a_0 c_0^z \tan\left(\frac{\pi\, z}{2}\right) \left(-\nabla^2\right)^{\frac{z+1}{2}-1} \tag{8}$$

Since the problem is nonlinear, it is necessary to compute the energy deposition rate for different harmonics, that is, to consider attenuations and acoustic pressures for frequencies that are integer multiples of the fundamental frequency. Hence, the energy deposition rate can be calculated by (9), where N represents the number of harmonics considered (Khokhlova *et al.*, 2006; Suomi *et al.*, 2017).

$$Q = \sum_{n=1}^{N} a(f_n) \frac{p_n^2}{\rho_0 c_0} \tag{9}$$

Therefore, for the acoustic problem, the main objective is to obtain, through equations (5), (6) and (7) and associated boundary and initial conditions, the acoustic pressure field in the domain. Boundary and initial conditions will be discussed later in the paper. With this pressure distribution, it is possible to calculate the energy deposition rate with equation (9), thus enabling the analysis of the thermal problem.

Simulations performed here consider a 2D rectangular domain with dimensions 45 mm x 45 mm, as illustrated by figure 1. The region consists of several layers, including water (light blue), skin (epidermis, dermis and hypodermis) and muscle, with thicknesses of 26 mm, 0.1 mm, 1.5 mm, 4 mm and 13 mm respectively. A rectangular-shaped region

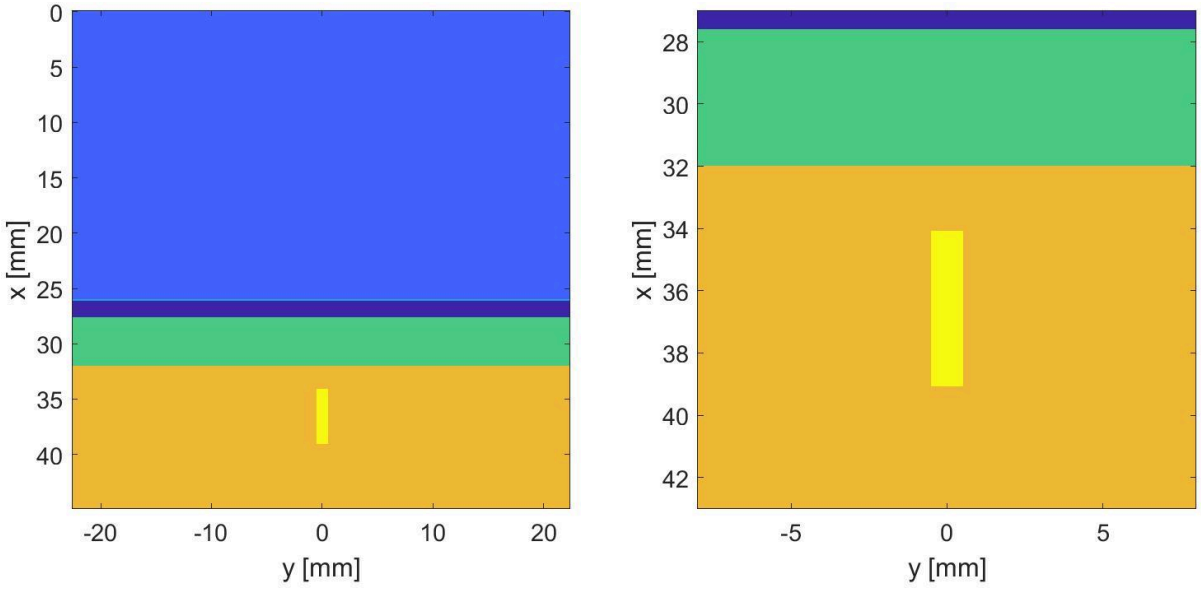

(a) (b)

Figure 1: (a) Numerical domain. (b) Enlargement around the tumor

represents the tumor to be treated with HIFU thermal ablation. The tumor is assumed with dimensions 1 mm x 5 mm and is located at the ultrasound axis ($y = 0$) in the muscle. The focal point of the ultrasound transducer considered in the simulations coincides with the center of the rectangular tumor. Figure 1b presents an enlargement of figure 1a around the tumor.

For the cases examined here, it was observed that the magnitude of the fourth harmonic was very small when compared to the first three harmonics. Hence, the summation in equation (9) was limited to $N = 3$. After a grid convergence analysis, the region presented by figure 1a was discretized with a grid of 216 x 216 nodes, resulting in a spatial resolution of approximately 0.21 mm, which was sufficient to resolve the frequencies of all harmonics. A SU-142 Sonic Concepts (Sonic Concepts, 2019) transducer model, with radius $r = 35$ mm and diameter $D = 33$ mm, operating at a fundamental frequency $f_0 = 1.1$ MHz was considered. The resulting source pressure distribution is a sinusoidal continuous wave, which results in an acoustic power $P = 15$ W.

When analyzing high frequency sinusoidal signals, it is observed that classical numerical techniques, such as the finite difference method, require around 10 points per wavelength to obtain a good accuracy, which results in an extremely high computational demand for conventional computers. The k-Wave MATLAB toolbox used in this work solves the equations that govern the problem using the pseudospectral k-space method, where spatial derivatives are calculated by the Collocation Spectral Method (Bojarski, 1982; Treeby *et al.*, 2011). This enables the use of approximately 3 points per wavelength, which considerably reduces the computational time.

For the boundary conditions of the acoustic problem, it was considered the use of Perfectly Matched Layers (PML) at all surfaces. This kind of boundary condition simulates a medium without reflections or incoming fluxes (Berenger, 1994; Gedney, 1996). The physical properties of the medium considered for the acoustic simulation are indicated in table 1 (Duck, 2013).

Table 1: Medium properties for the acoustic problem (Duck, 2013)

	Water	Epidermis	Dermis	Hypodermis	Muscle	Tumor
c_0 (m/s)	1500	1480	1480	1480	1580	1560
ρ_0 (kg/m^3)	1000	1100	1100	970	1070	1070
a_0 (dB/cmMHz$^{1.2}$)	0.0022	0.6000	0.6000	0.6000	0.6700	0.6700
B/A	5.20	7.87	7.87	10.00	7.43	7.43

For the acoustic simulations, steady state was reached in 50 μs. Then, the acoustic pressures of each harmonic in the region were saved, thus enabling the calculation of the energy deposition in the region and the analysis of the heat transfer problem.

3. BIOHEAT TRANSFER PROBLEM

Although many bioheat transfer problems have been proposed in the literature, Pennes' model, as shown in equation (10), is still widely used for cases that do not involved analyses near large blood vessels. In this model, subscript b represents the blood, c is the specific heat, w is the perfusion rate and Q_m, the metabolic heat generation rate (Pennes, 1948).

$$\rho_0 c \frac{\partial T}{\partial t} = \nabla \cdot (k \nabla T) + w_b \rho_b c_b (T_b - T) + Q + Q_m \tag{10}$$

In this work involving HIFU heating, the energy deposition rate is very large when compared to the heat sources due to metabolism and blood perfusion. Therefore, these quantities are neglected in the foregoing analysis, and the thermal problem is modeled by:

$$\rho_0 c \frac{\partial T}{\partial t} = \nabla \cdot (k \nabla T) + Q \tag{11}$$

It was considered that the water and biological tissue layers were at the uniform initial temperatures of 25 °C and 37 °C, respectively. These temperatures were then also assumed to be the boundary conditions for the problem. Once the solution of (11) is obtained, it is possible to estimate, with the local transient temperature variation, the thermal damage to the tissue. The Arrhenius model for calculating thermal damage (12) is used in this work, where A indicates a frequency factor, E_a, the activation energy, and R is the universal gas constant (Henriques Jr and Moritz, 1947; Wright, 2003).

$$\Omega = \int_0^{t'} A \exp\left(-\frac{E_a}{RT}\right) dt \tag{12}$$

According to Henriques Jr and Moritz (1947), first-degree burns occur for $\Omega = 0.53$, while second-degree burns occur for $\Omega = 1$. It was suggested that, for $\Omega = 10^4$, third-degree burns would occur (Takata, 1974). For the calculation of Ω, the parameters used were $A = 1.82 \times 10^{51}$ s^{-1}, $E_a = 3.27 \times 10^5$ J/mol and $R = 8.31$ J/molK (Weaver and Stoll, 1967). The medium properties used for the heat transfer simulation are presented by table 2.

Table 2: Medium properties for the heat transfer simulation (Duck, 2013)

	Water	Epidermis	Dermis	Hipodermis	Muscle	Tumor
c (J/kg°C)	4200	3600	3600	3600	3630	3630
k (W/m°C)	0,61	0,29	0,29	0,29	0,51	0,51

4. OPTIMIZATION

During the numerical simulations performed in this work, it was noticed that the region affected by the treatment strongly depends on the power of the transducer and the heating time. For the results presented above, values were fixed for these two parameters. On the other hand, it is of great practical interest to find optimum values for these parameters, so that a pre-specified region of damaged tissue is imposed.

In order to estimate optimum acoustic power and heating time values, an optimization study was then conducted within the Bayesian framework of statistics, to take into account prior information for the model parameters and acceptable uncertainties for the damaged region (Kaipio and Fox, 2011). For the solution of an inverse problem within the Bayesian framework of statistics, the formal mechanism to combine the new measurements information with the previously available information is Bayes' theorem, given by (13). In this relation, $\pi_{\text{posterior}}(\mathbf{P})$ is the posterior probability density, $\pi(\mathbf{P})$ is the prior density, $\pi(\mathbf{Y}|\mathbf{P})$ is the likelihood function and $\pi(\mathbf{Y})$ is the marginal probability density of the measurements, which plays the role of a normalizing constant. Here, for the solution of the optimization problem, the vector $\mathbf{Y}$ contains the desired thermal damage in the region at the end of the heating period and the likelihood represents the aimed distribution of this quantity.

$$\pi_{\text{posterior}}(\mathbf{P}) = \pi(\mathbf{P}|\mathbf{Y}) = \frac{\pi(\mathbf{Y}|\mathbf{P})\pi(\mathbf{P})}{\pi(\mathbf{Y})} \tag{13}$$

In this work, the posterior distribution is explored by using the Metropolis-Hastings algorithm of the Markov chain Monte Carlo (MCMC) method (Kaipio and Fox, 2011; Kaipio and Somersalo, 2006; Metropolis *et al.*, 1953; Alaeian *et al.*,

2018; Alaeian and Orlande, 2017). The implementation of the Metropolis-Hastings algorithm starts with the selection of a proposal distribution $q(\mathbf{P}^*|\mathbf{P}^{(t)})$, which is used to draw a new candidate state $\mathbf{P}^*$, given the current state $\mathbf{P}^{(t)}$ of the Markov chain. In order to avoid eventual cases where $\pi_{\text{posterior}}(\mathbf{P}^{(t)})q(\mathbf{P}^*|\mathbf{P}^{(t)}) > \pi_{\text{posterior}}(\mathbf{P}^*)q(\mathbf{P}^{(t)}|\mathbf{P}^*)$, that is, the process moves from $\mathbf{P}^{(t)}$ to $\mathbf{P}^*$ more often than the reverse, a probability $\psi(\mathbf{P}^*|\mathbf{P}^{(t)})$ is introduced so that the reversibility condition is satisfied. This relation can be represented by (14).

$$\pi_{\text{posterior}}(\mathbf{P}^{(t)})q(\mathbf{P}^*|\mathbf{P}^{(t)})\psi(\mathbf{P}^*|\mathbf{P}^{(t)}) = \pi_{\text{posterior}}(\mathbf{P}^*)q(\mathbf{P}^{(t)}|\mathbf{P}^*) \tag{14}$$

Therefore, $\psi(\mathbf{P}^*|\mathbf{P}^{(t)})$ can be expressed by (15), also called the Metropolis-Hastings ratio, where $\psi(\mathbf{P}^*|\mathbf{P}^{(t)}) = 1$ when $\pi_{\text{posterior}}(\mathbf{P}^{(t)}q(\mathbf{P}^*|\mathbf{P}^{(t)}) = \pi_{\text{posterior}}(\mathbf{P}^*)q(\mathbf{P}^{(t)}|\mathbf{P}^*)$.

$$\psi(\mathbf{P}^*|\mathbf{P}^{(t)}) = \min\left[1, \frac{\pi_{\text{posterior}}(\mathbf{P}^*)q(\mathbf{P}^{(t)}|\mathbf{P}^*)}{\pi_{\text{posterior}}(\mathbf{P}^{(t)})q(\mathbf{P}^*|\mathbf{P}^{(t)})}\right] \tag{15}$$

The Metropolis-Hastings algorithm can then be summarized by the following steps Metropolis *et al.* (1953):

1. Let $t = 1$ and start the Markov chain with the initial state $\mathbf{P}^{(1)}$.
2. Sample a candidate point $\mathbf{P}^*$ from a proposal distribution $q(\mathbf{P}^*|\mathbf{P}^{(t)})$.
3. Calculate the probability $\psi(\mathbf{P}^*|\mathbf{P}^{(t)})$ with equation (15).
4. Generate a random value $U(0,1)$, which is uniformly distributed in $(0,1)$.
5. If $U(0,1) \leq \psi(\mathbf{P}^*|\mathbf{P}^{(t)})$, set $\mathbf{P}^{(t+1)} = \mathbf{P}^*$. Otherwise, set $\mathbf{P}^{(t+1)} = \mathbf{P}^{(t)}$.
6. Make $t = t + 1$ and return to step 2 in order to generate the sequence $\mathbf{P}^{(1)}, \mathbf{P}^{(2)}, ..., \mathbf{P}^{(n)}$.

In this way, a sequence is generated to represent the posterior distribution and inference on this distribution is obtained from inference on the samples $\mathbf{P}^{(1)}, \mathbf{P}^{(2)}, ..., \mathbf{P}^{(n)}$. We note that values of $\mathbf{P}^{(t)}$ must be ignored until the chain has not converged to equilibrium (the burn-in period).

For the results presented below, priors for the model parameters and likelihood were assumed Gaussian. The model parameters were assumed independent. The priors were centered at the values presented by table 1, with relative standard deviations of 10^{-4} and 0.05. The largest standard deviation was applied only to the heating time and transducer power, which were the focus of this work. The Gaussian likelihood was centered at unitary values inside the tumor and null values in the remaining region. This optimal solution was considered acceptable with standard deviations of 10^{-3}.

5. RESULTS AND DISCUSSIONS

Figure 2 shows the acoustic pressures for each of the three harmonics used in the analysis, along the x direction on the axis of the transducer ($y = 0$). We notice that the magnitude of the third harmonic is already quite small as compared to the first harmonic. The steady state RMS pressure distribution and energy deposition rate are presented by figures 3a and 3b, respectively. These figures show the larger heat source term in the tumor region, as a result of an adequate transducer location.

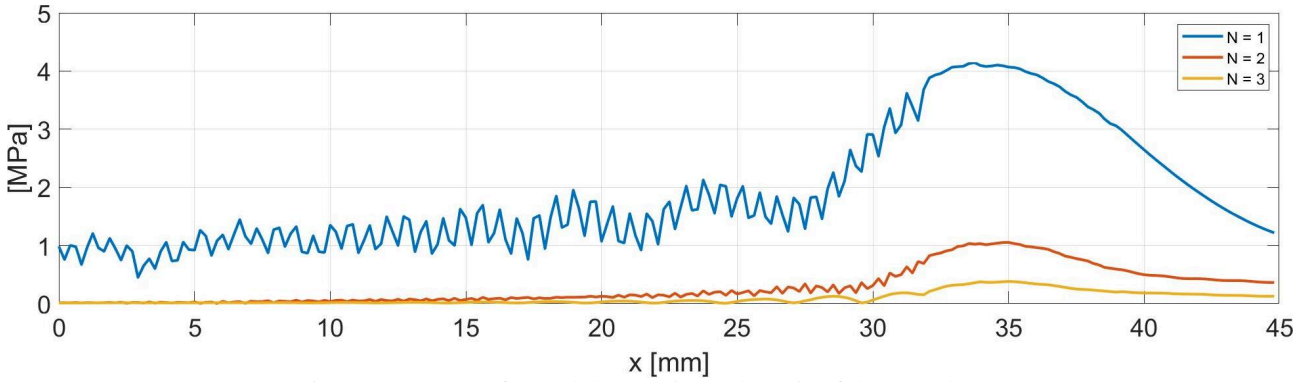

Figure 2: Pressure for each harmonic on the axis of the transducer.

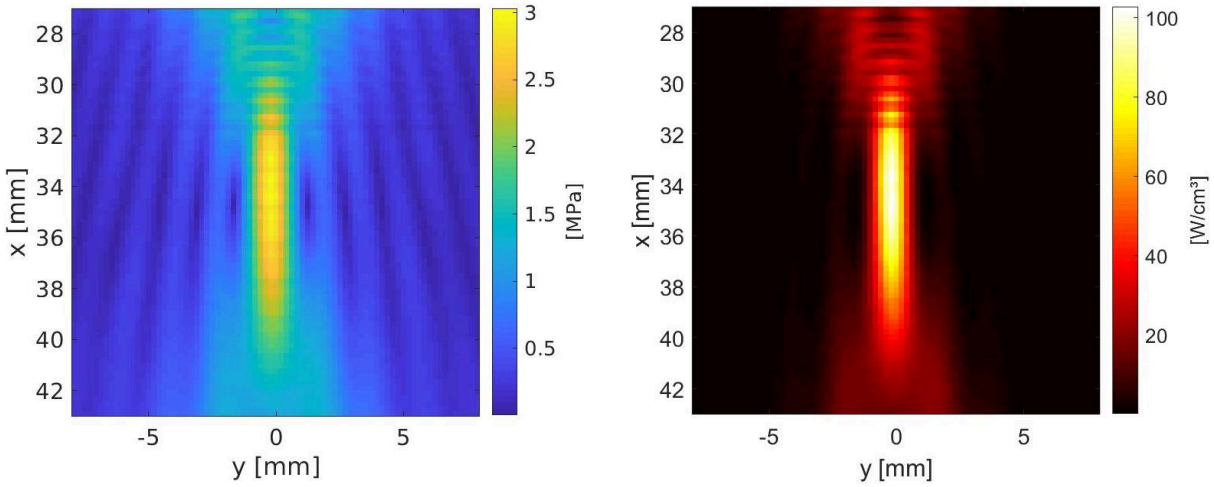

(a) (b)

Figure 3: (a) RMS pressure. (b) Energy deposition rate.

The bioheat problem was numerically solved by finite differences, considering the heating and cooling times equal to 2 seconds and 90 seconds, respectively. The value of the thermal damage Ω was then calculated as post-processing of the temperature variation in the region, which made it possible to estimate the region affected by the treatment. Figure 4 illustrates the temperature distributions of the bioheat transfer simulation. The temperatures in the region at the end of the heating period (figure 4a) shows that the tumor was heated to about 75 °C and heat is diffused to the surrounding regions, which also reached large temperatures. The temperature fast decays after the heating is stopped, as presented by figure 4b.

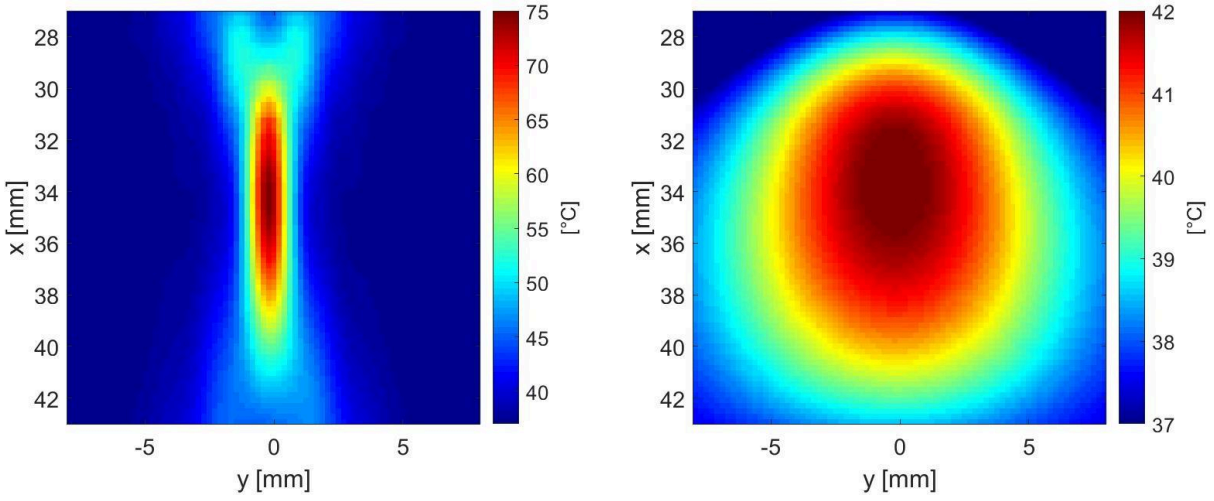

(a) (b)

Figure 4: Temperature distributions: (a) after heating period of 2 seconds; (b) after cooling period of 90 seconds.

Thermal damage was concentrated to the tumor region, as shown by figure 5a. Figure 5b is an estimation of the region affected by the heat, where the green region represents first-degree burn ($0.53 \leq \Omega < 1$) and the red region represents second-degree burn ($\Omega \geq 1$). The computer code developed in MATLAB for the finite difference solution of the bioheat transfer problem was verified by using an analytic solution for a homogeneous medium, obtained with the Classical Integral Transform Technique (CITT) (Özışık, 1993; Mikhailov and Cotta, 1994). This verification procedure is omitted here for the sake of brevity.

Figure 6 illustrates the Markov chains obtained with the Metropolis-Hastings algorithm for both acoustic power and heating time. As expected, this figure shows a strong correlation between the chains for these two parameters, which is evident from the fact that the heating time increases when the acoustic power decreases. Moreover, there are periods when the chains reach different equilibrium distributions. Means of these equilibrium distributions are shown by lines of different colors. The different equilibrium distributions correspond to multiple solutions of the optimization problem that satisfy the aimed likelihood function. Means and standard deviations of the three equilibrium distributions observed in figures 6a and 6b are presented in table 3.

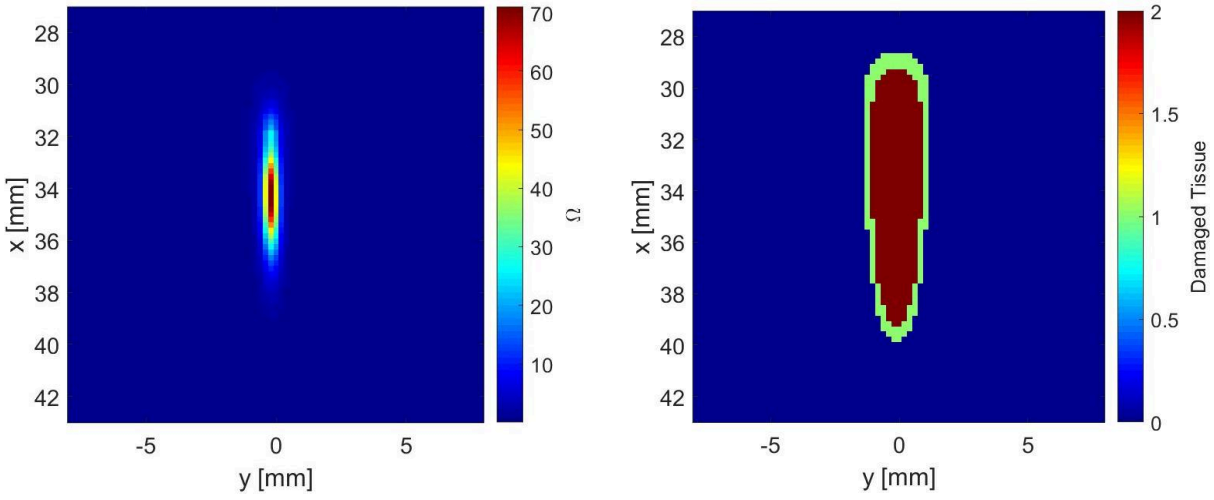

(a) (b)

Figure 5: (a) Thermal damage. (b) Regions corresponding to $0.53 \leq \Omega < 1$ and $\Omega \geq 1$ marked in green and red, respectively.

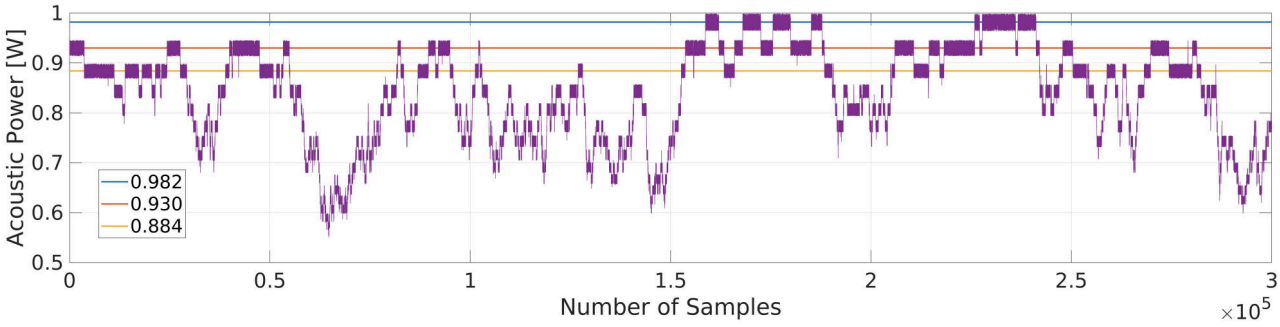

(a)

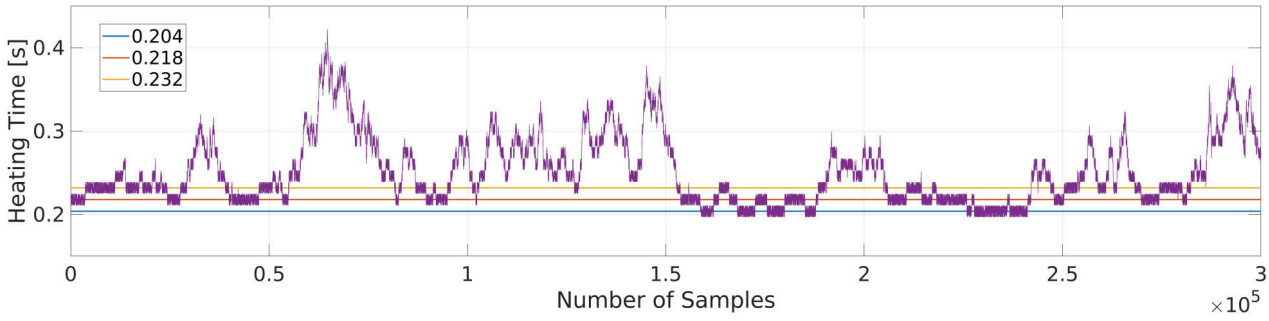

(b)

Figure 6: Markov chains for (a) acoustic power and (b) heating time.

Table 3: Means and standard deviations of the equilibrium distributions

	Acoustic Power [W]		Heating Time [s]	
	Mean	Standard Deviation	Mean	Standard Deviation
Equilibrium distribution 1	0.982	0.0098	0.204	0.0040
Equilibrium distribution 2	0.930	0.0094	0.218	0.0041
Equilibrium distribution 3	0.884	0.0086	0.232	0.0039

The resulting thermal damages obtained with the means presented in table 3 are shown in figures 7a, 8a and 9a, respectively, while the absolute differences between these values are shown in figure 10. The regions corresponding to $\Omega \geq 1$ are shown in figures 7b, 8b and 9b, respectively. These figures show that the optimized thermal damages are very well restricted to the tumor region, as desired.

The computational cost for the optimization problem with the Metropolis-Hastings algorithm was about 48 hours, for a MATLAB code running in a computer with a Core i7 processor and 8 GB of RAM memory. Spatial grid resolution was reduced for these results, in order to reduce the associated computation time required for the implementation of MCMC.

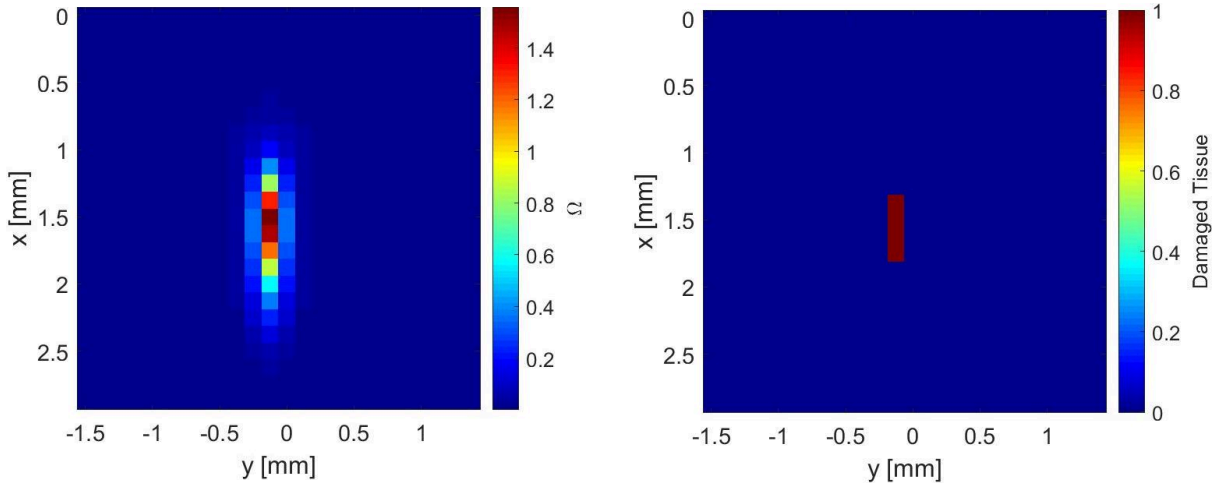

(a) (b)

Figure 7: Results for equilibrium distribution 1. (a) Thermal damage. (b) Region corresponding to $\Omega \geq 1$ marked in red.

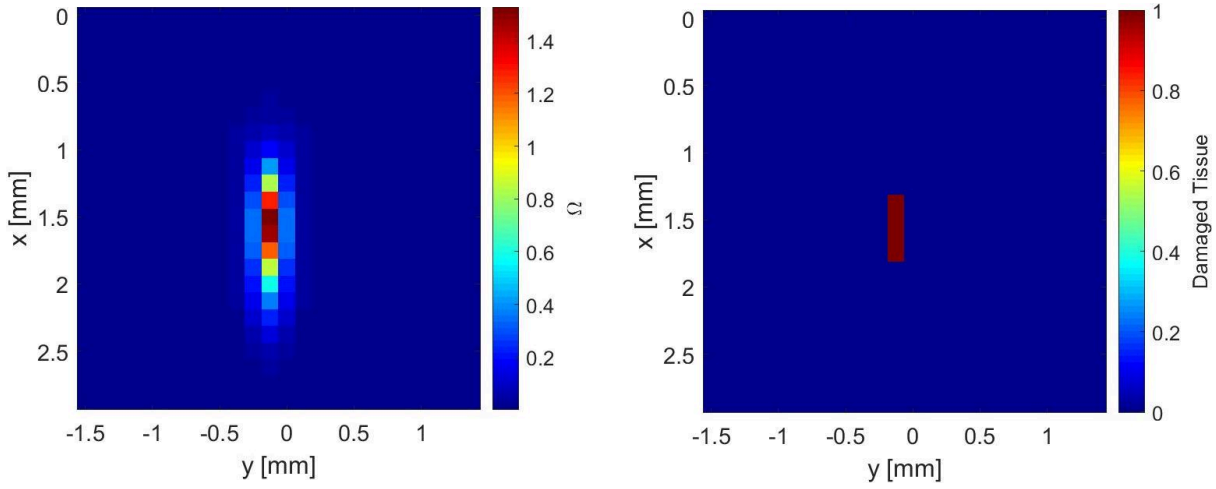

(a) (b)

Figure 8: Results for equilibrium distribution 2. (a) Thermal damage. (b) Region corresponding to $\Omega \geq 1$ marked in red.

6. CONCLUSIONS

This work presented the numerical simulation and the optimization under uncertainties of thermal ablation of a tumor, with heating imposed by high intensity focused ultrasound (HIFU). The acoustic problem was solved with the k-Wave MATLAB toolbox, while the bioheat transfer equation was solved with finite differences. For the optimization under uncertainties, we considered the Markov chain Monte Carlo method, implemented via the Metropolis-Hastings algorithm.

Although it is evident that, for real applications, a considerable computational power is required for MCMC, this study shows that it is possible to estimate the optimum parameters for the imposed damaged region. The results presented above were focused on the optimum values of heating time and transducer power. The continuation of this work shall involve larger uncertainties for other model parameters, in special the physical properties, which can vary from individual to individual, and even for the same individual with different physiological conditions.

7. ACKNOWLEDGMENTS

The support provided by CNPq, CAPES, and FAPERJ, agencies of the Brazilian government, is greatly appreciated.

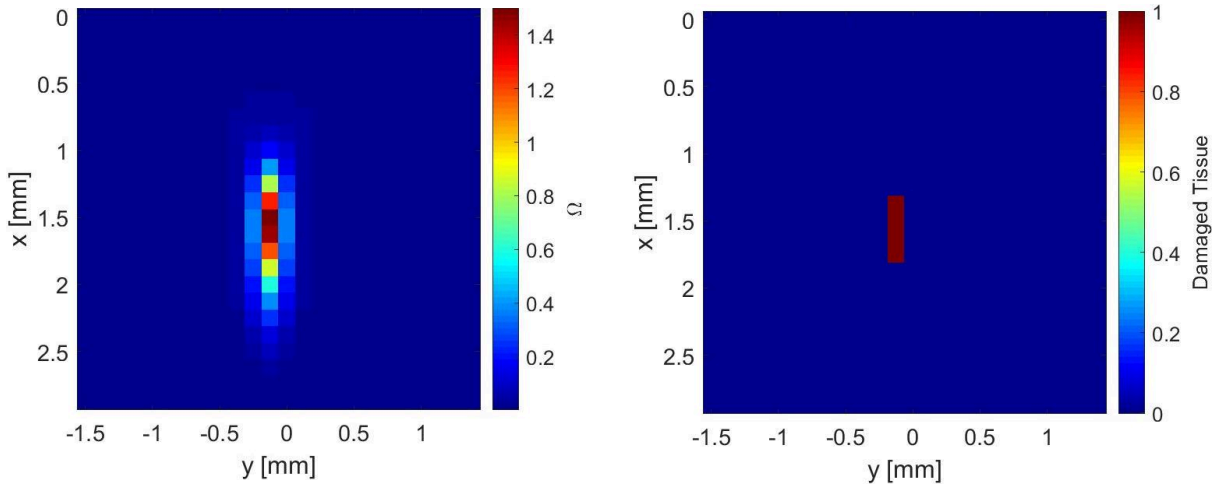

(a) (b)

Figure 9: Results for equilibrium distribution 3. (a) Thermal damage. (b) Region corresponding to $\Omega \geq 1$ marked in red.

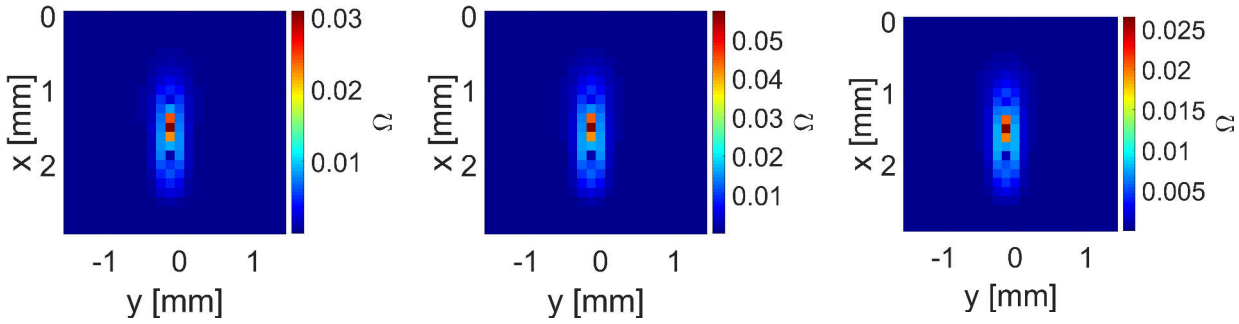

(a) (b) (c)

Figure 10: Absolute difference between thermal damages for equilibrium distributions: (a) 1 and 2; (b) 1 and 3; (c) 2 and 3.

8. REFERENCES

Alaeian, M. and Orlande, H.R.B., 2017. "Inverse photoacoustic technique for parameter and temperature estimation in tissues". *Heat Transfer Engineering*, Vol. 38, No. 18, pp. 1573–1594.

Alaeian, M., Orlande, H.R.B. and Lamien, B., 2018. "Application of the photoacoustic technique for temperature measurements during hyperthermia". *Inverse Problems in Science and Engineering*, pp. 1–21.

Berenger, J.P., 1994. "A perfectly matched layer for the absorption of electromagnetic waves". *Journal of computational physics*, Vol. 114, No. 2, pp. 185–200.

Bojarski, N.N., 1982. "The k-space formulation of the scattering problem in the time domain". *The Journal of the Acoustical Society of America*, Vol. 72, No. 2, pp. 570–584.

Duck, F.A., 2013. *Physical properties of tissues: a comprehensive reference book*. Academic press.

Gedney, S.D., 1996. "An anisotropic perfectly matched layer-absorbing medium for the truncation of fdtd lattices". *IEEE transactions on Antennas and Propagation*, Vol. 44, No. 12, pp. 1630–1639.

Haugen, B.R., Alexander, E.K., Bible, K.C., Doherty, G.M., Mandel, S.J., Nikiforov, Y.E., Pacini, F., Randolph, G.W., Sawka, A.M., Schlumberger, M. *et al.*, 2016. "2015 american thyroid association management guidelines for adult patients with thyroid nodules and differentiated thyroid cancer: the american thyroid association guidelines task force on thyroid nodules and differentiated thyroid cancer". *Thyroid*, Vol. 26, No. 1, pp. 1–133.

Henriques Jr, F. and Moritz, A., 1947. "Studies of thermal injury: I. the conduction of heat to and through skin and the temperatures attained therein. a theoretical and an experimental investigation". *The American journal of pathology*, Vol. 23, No. 4, p. 530.

Hill, C. and Ter Haar, G., 1995. "High intensity focused ultrasound—potential for cancer treatment". *The British journal of radiology*, Vol. 68, No. 816, pp. 1296–1303.

Kaipio, J. and Somersalo, E., 2006. *Statistical and computational inverse problems*, Vol. 160. Springer Science & Business Media.

Kaipio, J.P. and Fox, C., 2011. "The bayesian framework for inverse problems in heat transfer". *Heat Transfer Engineer-*

ing, Vol. 32, No. 9, pp. 718–753.

Kennedy, J.E., Ter Haar, G. and Cranston, D., 2003. "High intensity focused ultrasound: surgery of the future?" *The British journal of radiology*, Vol. 76, No. 909, pp. 590–599.

Khokhlova, V.A., Bailey, M.R., Reed, J.A., Cunitz, B.W., Kaczkowski, P.J. and Crum, L.A., 2006. "Effects of nonlinear propagation, cavitation, and boiling in lesion formation by high intensity focused ultrasound in a gel phantom". *The Journal of the Acoustical Society of America*, Vol. 119, No. 3, pp. 1834–1848.

Kinsler, L.E., Frey, A.R., Coppens, A.B. and Sanders, J.V., 1999. "Fundamentals of acoustics". *Fundamentals of Acoustics, 4th Edition, by Lawrence E. Kinsler, Austin R. Frey, Alan B. Coppens, James V. Sanders, pp. 560. ISBN 0-471-84789-5. Wiley-VCH, December 1999.*, p. 560.

Metropolis, N., Rosenbluth, A.W., Rosenbluth, M.N., Teller, A.H. and Teller, E., 1953. "Equation of state calculations by fast computing machines". *The journal of chemical physics*, Vol. 21, No. 6, pp. 1087–1092.

Mikhailov, M. and Cotta, R., 1994. "Integral transform solution of eigenvalue problems". *Communications in numerical methods in engineering*, Vol. 10, No. 10, pp. 827–835.

Özışık, M.N., 1993. *Heat conduction*. John Wiley & Sons.

Pennes, H.H., 1948. "Analysis of tissue and arterial blood temperatures in the resting human forearm". *Journal of applied physiology*, Vol. 1, No. 2, pp. 93–122.

Sonic Concepts, 2019. "SU-Transducer Series 33 mm". `http://sonicconcepts.com/wp-content/uploads/2016/05/SU-%C3%9833-mm_DataSheet_v2.pdf`.

Suomi, V., Jaros, J., Treeby, B. and Cleveland, R.O., 2017. "Full modeling of high-intensity focused ultrasound and thermal heating in the kidney using realistic patient models". *IEEE Transactions on Biomedical Engineering*, Vol. 65, No. 5, pp. 969–979.

Szabo, T.L., 1995. "Causal theories and data for acoustic attenuation obeying a frequency power law". *The Journal of the Acoustical Society of America*, Vol. 97, No. 1, pp. 14–24.

Takata, A., 1974. "Development of criterion for skin burns". *Aerospace Medicine*, Vol. 45, No. 6, pp. 634–637.

Treeby, B.E. and Cox, B.T., 2010. "k-wave: Matlab toolbox for the simulation and reconstruction of photoacoustic wave fields". *Journal of biomedical optics*, Vol. 15, No. 2, p. 021314.

Treeby, B.E., Jaros, J., Rendell, A.P. and Cox, B., 2012. "Modeling nonlinear ultrasound propagation in heterogeneous media with power law absorption using ak-space pseudospectral method". *The Journal of the Acoustical Society of America*, Vol. 131, No. 6, pp. 4324–4336.

Treeby, B.E., Tumen, M. and Cox, B.T., 2011. "Time domain simulation of harmonic ultrasound images and beam patterns in 3d using the k-space pseudospectral method". In *International Conference on Medical Image Computing and Computer-Assisted Intervention*. Springer, pp. 363–370.

Tunbridge, W., Evered, D., Hall, R., Appleton, D., Brewis, M., Clark, F., Evans, J.G., Young, E., Bird, T. and Smith, P., 1977. "The spectrum of thyroid disease in a community: the whickham survey". *Clinical endocrinology*, Vol. 7, No. 6, pp. 481–493.

Vander, J.B., Gaston, E.A. and Dawber, T.R., 1968. "The significance of nontoxic thyroid nodules: final report of a 15-year study of the incidence of thyroid malignancy". *Annals of internal medicine*, Vol. 69, No. 3, pp. 537–540.

Weaver, J.A. and Stoll, A.M., 1967. "Mathematical model of skin exposed to thermal radiation". Technical report, NAVAL AIR DEVELOPMENT CENTER WARMINSTER PA AEROSPACE MEDICAL RESEARCH DEPT.

Wright, N.T., 2003. "On a relationship between the arrhenius parameters from thermal damage studies". *Journal of biomechanical engineering*, Vol. 125, No. 2, pp. 300–304.

9. RESPONSIBILITY NOTICE

The authors are solely responsible for the printed material included in this paper.